HHS Public Access

Author manuscript

J Orthop Res. Author manuscript; available in PMC 2016 May 01.

Published in final edited form as:

J Orthop Res. 2016 May ; 34(5): 845–851. doi:10.1002/jor.23080.

Antioxidant Impregnated Ultra-High Molecular Weight Polyethylene Wear Debris Particles Display Increased Bone Remodeling and a Superior Osteogenic:Osteolytic Profile vs. Conventional UHMWPE Particles in a Murine Calvaria Model

Yu Chen[1,2], **Nadim J. Hallab**[3], **Yen-Shuo Liao**[4], **Venkat Narayan**[4], **Edward M. Schwarz**[1,2,5], and **Chao Xie**[1,2]

[1]Center for Musculoskeletal Research, University of Rochester School of Medicine and Dentistry, Rochester, NY 14642

[2]Department of Orthopaedics, University of Rochester School of Medicine and Dentistry, Rochester, NY 14642

[3]Department of Orthopaedics, Rush University, 1735 W Harrison, Chicago, IL 60612

[4]DePuy, Johnson & Johnson Inc., 700 Orthopaedic Drive, Warsaw, IN 46581

Abstract

Periprosthetic osteolysis remains a major limitation of long-term successful total hip replacements with ultra-high molecular weight polyethylene (UHMWPE) bearings. As intra and extracellular reactive oxygen species are know to contribute to wear debris-induced osteoclastic bone resorption and decreased osteoblastic bone formation, antioxidant doped UHMWPE has emerged as an approach to reduce the osteolytic potential of wear debris and maintain coupled bone remodeling. To test this hypothesis in vivo, we evaluated the effects of crosslinked UHMWPE wear debris particles (AltrX™), versus similar wear particles made from COVERNOX™ containing UHMWPE (AOX™), in an established murine calvaria model. Eight-week-old female C57B/6 mice (n=10/Group) received a pre-op micro-CT scan prior to surgical implantation of the UHMWPE particles (2mg), or surgery without particles (sham). Dynamic labeling was performed by intraperitoneal injection of calcein on day 7 and alizarin on day 9, and the calvaria were harvested for micro-CT and histology on day 10. Surprisingly, we found that AOX particles induced significantly more bone resorption (1.72-fold) and osteoclast numbers (1.99-fold) vs. AltrX ($p<0.001$). However, AOX also significantly induced 1.64-fold more new bone formation vs. AltrX ($p<0.01$). Moreover, while the osteolytic:osteogenic ratio of both particles was very close to 1.0, which is indicative of coupled remodeling, AOX was more osteogenic (Slope=1.13±0.10 vs. 0.97±0.10). Histomorphometry of the metabolically labeled undecalcified calvaria revealed a consistent trend of greater MAR in AOX vs. AltrX. Collectively, these results demonstrate that anti-oxidant

[5]To whom correspondence should be addressed: Dr. Edward M. Schwarz, The Center for Musculoskeletal Research, University of Rochester Medical Center, 601 Elmwood Avenue, Box 665, Rochester, NY 14642, Phone 585-275-3063, FAX 585-275-1121, Edward_Schwarz@URMC.Rochester.edu.

Author Contributions Statement: All authors have contributed to: [1] the research design, and/or the acquisition, analysis or interpretation of data; [2] drafting the paper or revising it critically; and [3] approval of the submitted and final versions.

impregnated UHMWPE particles have decreased osteolytic potential due to their increased osteogenic properties that support coupled bone remodeling.

Keywords

UHMWPE; Antioxidant; Wear debris; Osteolysis; Osteogenesis; Bone Remodeling; Murine model

Introduction

Total hip replacement (THR) is a common procedure performed for end stage osteoarthritis, rheumatoid arthritis, avascular necrosis of the hip, and femoral neck fractures. Although long-term THR outcomes with ultra-high molecular weight polyethylene (UHMWPE) bearing surfaces are known to be limited by wear debris and subsequent periprosthetic osteolysis, this construct remains a popular implant design based on its consistent results and survivorship of ~85% after 15 years [1], and the significant pitfalls of alternative articulation designs (i.e. metal-on-metal and ceramic-on-ceramic) [2; 3]. Therefore, the field has been working on biomaterial modifications to UHMWPE that will decrease particle-induced inflammation, osteoclastogenesis, and uncoupled bone resorption, which is known to be the cause of periprostetic osteolysis and aseptic loosening [4–11].

Reactive oxygen species (ROS) are a dominant contributor to wear debris-induced osteolysis [12]. The ROS in this process is derived from multiple sources. Ititially, it can be produced from the free radicals trapped in the final UHMWPE product after gamma irradiation, which are liberated during particle generation [13]. Additionally, ROS is generated by macrophages during normal and “frustrated phagocytosis” of UHMWPE particles, and the subsequent pro-inflammatory cascade [12]. Furthermore, ROS also directly excacerbates osteolysis by inducing osteoclastognesis, increasing osteoclastic resorption and inhibition osteoblast diferention and bone formation[12; 14; 15]. Interestingly, biomaterial research in this field has also focused on ROS, and antioxidants such as vitamin E have been incorporated into UHMWPE resin [16], or introduced by diffusing them into already consolidated and radiated UHMWPE [17], to decrease the oxidation of the material itself. Considering this convergence of inflammatory bone loss and biomaterial research, we proposed that the antioxidants present in antioxidant-stabilized UHMWPE wear debris to promote a more favorable host response [18], even though direct evidence of antioxidant distribution away from the polymerized material has yet to be demonstrated. Now that these products are approaching clinical use, formal evaluations of the osteolytic and osteogenic potential of UHMWPE particles with and without antioxidants in head-to-head in vivo studies are warranted. To this end, we recently modified a well-established murine calvaria model of wear debris-induced osteolysis[19], and incorporated longitudinal micro-CT [20], to derived volumetric outcomes of osteolysis and osteogenesis [18]. Moreover, preliminary results in this model demonstrated that antioxidants enhance bone formation in response to particle-induced bone resorption [18]. Based on these findings, here we present a formal head-to-head study to testing the hypothesis that UHMWPE particles impregnated with the antioxidant COVERNOX™ (DePuy Synthes Joint Reconstruction), have decrease osteolytic potential and increased osteogenic potential, versus unimpregnated particles of similar UHMWPE

chemistry, size distribution and shape, in the murine calvaria model of wear debris-induced bone resorption.

Materials and Methods

The ultra high molecular weight polyethylene (UHMWPE) bearing materials used in the study are: 1) Virgin GUR 1020 UHMWPE, containing no antioxidants, is consolidated by ram extrusion, irradiated to a gamma radiation dose of 75 kGy and subsequently remelted to quench residual free radicals, machined into acetabular bearings, cleaned, packaged and terminally sterilized by gas plasma to yield AltrX™ (DePuy Synthes Joint Reconstruction); and 2) Virgin GUR 1020 UHMWPE powder is compounded with a hindered phenol antioxidant, Pentaerythritol tetrakis [3-(3,5-di-tert-butyl-4-hydroxyphenyl) propionate] under the trade name COVERNOX™, consolidated by compression molding, radiation-crosslinked using a nominal gamma dose of 85 kGy, machined into acetabular bearings, cleaned, packaged and terminally sterilized using a nominal gamma dose of 30 kGy to yield AOX™ (DePuy Synthes Joint Reconstruction).

Wear debris particle generation

Particles from AltrX™ and AOX™ bearings were generated using high-speed cryomilling and cryopulverization (BioEngineering Solutions Inc., Chicago, IL) as previously described[20]. Particle filtering was used to isolate particles in the 1 to 10μm range, and they were characterized using low angle laser light scattering (Microtrac-X100), and scanning electron microscopy with EDS to confirm particle size, shape and composition. The major differential characteristics of these particles are summarized in Table 1. The particles were then EtO sterilized and verified to be free of endotoxins (<0.01uE, Kinetic QCL).

In vivo studies

All animal studies were performed under protocols approved by the University of Rochester Committee for Animal Resources as previously described [20]. Briefly, eight-week-old C57B/6 mice (n=10 per Group; 30 mice total) were shaved prior to calvaria surgery, and the area was sterilized with 70% ethanol and iodine. A 0.5×0.5-cm area of calvarial bone was exposed by making a midline sagittal incision over the calvaria, but leaving the periosteum intact to eliminate trauma-induced osteolysis and osteogenesis in response to bone injury, as we have observed in prior studies.[20; 21] A previously defined threshold dose of particles known to induce osteolysis (2mg) of AltrX or AOX,[18] were spread over the calvaria of each mouse, and the incision was closed with 2.0 interrupted sutures. A third group consisting of an incision of the skin only served as the Sham surgery control.

Micro-CT scanning and osteolysis vs. osteogenesis analysis

Micro-CT scans were performed with a VivaCT40 (ScanCo Medical, Basserdorf, Switzerland) using an isometric resolution of 15 μm. Baseline calvaria volume was obtained from in vivo scans on day 0 (before surgery), while the mice were anesthetized with 2% isofluorine and 1L/min oxygen. After sacrifice on day 10, the skulls were rescanned with the same parameters (n=10 per Group). The DICOM micro-CT files were then transferred to Amira ver. 5.4 (Visage Imaging, Inc., San Diego, CA) for quantitative analysis.

Quantification of the osteolytic and osteogenic volume was performed as previously described [18]. Briefly, the DICOM files were used to generate an initial 3D image of the calvaria at each time point, and these images were then imported into the Amira program for volumetric registration and analyses. Three distinct tissues types were defined based on their bone mineral density (BMD). In the region of interest (ROI), the original calvaria bone, which has a high BMD (zoom and data window = 1,000–7,000; display and masking = 1,700–7,000), was initially identified. Then an under-mineralized tissue with a lower BMD (zoom and data window = 1,000–3,000; display and masking = 1,000–2,500) was identified within the ROI, which we defined as new bone that formed in response to the wear debris-induced osteolysis. Finally, the unmineralized soft tissue (zoom and data window <1,000; display and masking <1,000), was identified within the ROI between the original calvaria was defined as osteolysis. Based on this tissue segmentation, we were able to calculate the Bone Resorption Volume and Bone Formation Volume for the three groups as illustrated in Figure 1.

Histomorphometry of osteoclast numbers and mineral apposition rate

After the ex vivo micro-CT scan, the calvaria were cut in half to allow for both demineralized (n=5 per Group) and undemineralized (n=5 per Group) histology as previously described [22; 23]. Bone remodeling was assessed from three contiguous 3 μm demineralized calvaria sections 500 μm apart stained with alcian blue hematoxylin/orange G (ABH/OG). Osteoclasts were quantified using the Visiopharm Image Analytical System (Version: 4.4.6.9) from three contiguous 3 μm demineralized sections 500μm apart stained for tartrate-resistant acid phosphatase (TRAP) using the Diagnostics Acid Phosphatase Kit (Sigma, St. Louis, MO, USA). Quantification of the mineral apposition rates (MAR) in the three groups of mice was performed on undemineralized sections, in which the distance between the calcein and alizarin labeled bone surfaces was determined as we have previously described [22].

Statistical analysis

Volumetric bone resorption, bone formation and osteoclasts are presented as means ± SD for each group, and statistical significance was determined using a one-way ANOVA with multiple comparison of Tukey of three treatment groups where $p<0.05$ was considered significant. The significance of the rank order of bone resorption volume versus bone formation volume was determined using the Wilcoxon rank-sum test. Correlations between osteolysis and osteogenesis were estimated using Pearson's correlation coefficient, and tested for significance using a two-sided *t*-test. The slope of the best-fit line and R^2 value was calculated with Prism software.

Results

Volumetric micro-CT analyses of the calvaria demonstrated that both AltrX and AOX particles induced significant bone resorption and bone formation versus Sham controls ($p<0.001$), which displayed minimal remodeling (Figure 2). Moreover, AOX particles stimulated a significant 1.72-fold increase in bone resorption, and a significant 1.64-fold increase in bone formation, versus AltrX particles ($p<0.001$). To further understand these

results, we performed a rank order evaluation of the particle-induced bone resorption and bone formation volumes (Figure 3A,B), and regression analyses to assess the osteolytic versus osteogenic potential of AltrX and AOX particles (Figure 3C,D). The Wilcoxon rank-sum tests confirmed that the AOX particles stimulate more bone resorption and bone formation by volume compared to AltrX particles ($p<0.002$). Furthermore, bone resorption volume correlated with bone formation, although the association was more significant in AltrX versus AOX particle treated calvaria ($R^2=0.70$, $p<0.0001$ vs. $R^2=2.16$, $p<0.001$). Finally, to assess the osteolytic:osteogenic potential of these particles directly, we determine the slope of the best-fit line in the regression graphs (Figure 3C,D), which demonstrated that both particles stimulate coupled bone remodeling, although AOX particles were more osteogenic versus AltrX (Slope=1.13 vs. Slope=0.97).

To confirm the micro-CT findings, histomorphometry was performed to quantify osteoclast numbers and mineral apposition rate (MAR), from decalcified and undecalcified tissue sections respectively. Alcian blue hematoxylin/orange G (ABH/OG) and tartrate resistant acid phosphatase (TRAP) stained demineralized histology of the calvaria confirmed the absence of bone remodeling in Sham controls, and extensive remodeling in particle treated calvaria (Figure 4). Furthermore, histomorphometry of the TRAP+ osteoclasts demonstrated that AOX particles induced significantly more osteoclasts than AltrX ($p<0.001$), which is consistent with the micro-CT. Finally, both particles significantly induced the MAR above the baseline level observed in Sham controls (Figure 5). Although it did not reach statistical significance due to variability, there was a trend of increased MAR in AOX versus AltrX particle treated calvaria ($p=0.2444$).

Discussion

Aseptic loosening of THR with UHMWPE bearing surfaces is largely caused by wear debris-induced periprothetic osteolysis [4–11]. However, it is important to note that this bone loss, which typically occurs over long periods of time (i.e. 5–10 years post-op), is biologically distinct from aggressive focal erosion observed in osteolytic bone cancer and osteomylitis. This is because under non-pathologic conditions, wear debris-induced bone resorption is coupled to bone formation, and results in homeostatic bone remodeling. Recent clinical studies on THR survivorship with UHMWPE bearing surfaces confirm excellent outcomes [24; 25]. In the case of AltrX with the PINNACLE acetabular cup, a 5-year survivorship of 97% for cementless THA was recently reported. However, there remains a small subset of patients that develop periprosthetic osteolysis and aseptic loosening [26–28]. The estabished paradigm to explain this dichotomy posits that aseptic loosing is due to an uncoupling of osteoclastic bone resorption and subsequent osteoblastic bone formation in the metablic processes, rather than a specific toxic UHMWPE wear debris responses. This theory is supported by longitudinal volumetric CT analysis of patients with varying degrees of periprosthetic bone loss [27–29]. Thus, it is based on this rationale that we deveolped longitudinal micro-CT as the primary outcome measure in our animal studies, as these quatitative biomarkers can directly measure coupled vs. uncoupled responses to wear debris. Indeed, in our first pilot study with these biomarkers we found that AOX induced more bone resorption and more bone formation than AltrX [18]. Thus, although the antioxidant UHMWPE particles exhibit an increased bone resorptive effect, their osteolytic potential is

offset by their increased osteogenic properties, which we confirmed here in a formal prospective study.

There are several important limitations to this initial proof of concept study that need to be recognized. The first is the murine calvaria model. Although this model has been utilized by many labs due to its cost-effectiveness, reproducibility and quantitative outcomes, it suffers from the absence of an implant and biomechanical forces that are central to aseptic loosening. Additionally, the periosteum-intact calvaria are flat bones that are distinct from reamed articulating long bones, which prostheses are implanted into. Another limitation of this study is the absence of formal dose-response experiments to validate our conclusions about the effects of the impregnated antioxidants, and to define the best dose of COVERNOX to be used in this UHMWPE material. These studies are ongoing, with the investigation of alterantive antioxidants (i.e. vitamine E), and UHMWPE compositions, with the goal of identifying the ideal combination for clinical use.

Acknowledgments

The authors would like to thank Sarah Mack and Michael Thullen for technical assistance with the histology and micro-CT analyses respectively. We also thank Todd Render for his helpful input. This work was supported by the National Institutes of Health PHS awards 1S10RR027340, P50 AR054041 and P30 AR061307; and DePuy J&J Inc.

References

1. Gomez-Barrena E, Medel F, Puertolas JA. Polyethylene oxidation in total hip arthroplasty: evolution and new advances. Open Orthop J. 2009; 3:115–120. [PubMed: 20111694]
2. Graves SE, Rothwell A, Tucker K, et al. A multinational assessment of metal-on-metal bearings in hip replacement. J Bone Joint Surg Am. 2012; 93(Suppl 3):43–47. [PubMed: 22262422]
3. Garcia-Cimbrelo E, Martinez-Sayanes JM, Minuesa A, et al. Mittelmeier ceramic-ceramic prosthesis after 10 years. J Arthroplasty. 1996; 11:773–781. [PubMed: 8934316]
4. Willert HG. Reactions of the articular capsule to wear products of artificial joint prostheses. J Biomed Mater Res. 1977; 11:157–164. [PubMed: 140168]
5. Harris WH. The problem is osteolysis. Clin Orthop. 1995:46–53. [PubMed: 7634590]
6. Trindade MC, Lind M, Sun D, et al. In vitro reaction to orthopaedic biomaterials by macrophages and lymphocytes isolated from patients undergoing revision surgery. Biomaterials. 2001; 22:253–259. [PubMed: 11197500]
7. Taki N, Tatro JM, Nalepka JL, et al. Polyethylene and titanium particles induce osteolysis by similar, lymphocyte-independent, mechanisms. J Orthop Res. 2005; 23:376–383. [PubMed: 15734251]
8. Wilkinson JM, Hamer AJ, Stockley I, et al. Polyethylene wear rate and osteolysis: critical threshold versus continuous dose-response relationship. J Orthop Res. 2005; 23:520–525. [PubMed: 15885470]
9. Purdue PE, Koulouvaris P, Potter HG, et al. The cellular and molecular biology of periprosthetic osteolysis. Clin Orthop Relat Res. 2007; 454:251–261. [PubMed: 16980902]
10. Yang SY, Yu H, Gong W, et al. Murine model of prosthesis failure for the long-term study of aseptic loosening. J Orthop Res. 2007; 25:603–611. [PubMed: 17278141]
11. Abu-Amer Y, Darwech I, Clohisy JC. Aseptic loosening of total joint replacements: mechanisms underlying osteolysis and potential therapies. Arthritis Res Ther. 2007; 9(Suppl 1):S6. [PubMed: 17634145]
12. Hallab NJ, Jacobs JJ. Biologic effects of implant debris. Bull NYU Hosp Jt Dis. 2009; 67:182–188. [PubMed: 19583551]

13. Jahan M, King M, Haggard W, et al. A study of long-lived free radicals in gamma-irradiated medical grade polyethlene. Radiat Phys Chem. 2001; 62:141–144.
14. Bax BE, Alam AS, Banerji B, et al. Stimulation of osteoclastic bone resorption by hydrogen peroxide. Biochem Biophys Res Commun. 1992; 183:1153–1158. [PubMed: 1567393]
15. D'Aiuto F, Nibali L, Parkar M, et al. Oxidative stress, systemic inflammation, and severe periodontitis. J Dent Res. 2010; 89:1241–1246. [PubMed: 20739696]
16. Lerf R, Zurbrugg D, Delfosse D. Use of vitamin E to protect cross-linked UHMWPE from oxidation. Biomaterials. 2010; 31:3643–3648. [PubMed: 20144479]
17. Oral E, Muratoglu OK. Vitamin E diffused, highly crosslinked UHMWPE: a review. Int Orthop. 2010; 35:215–223. [PubMed: 21120476]
18. Green JM, Hallab NJ, Liao YS, et al. Anti-oxidation Treatment of Ultra High Molecular Weight Polyethylene Components to Decrease Periprosthetic Osteolysis: Evaluation of Osteolytic and Osteogenic Properties of Wear Debris Particles in a Murine Calvaria Model. Current rheumatology reports. 2013; 15:325. [PubMed: 23532463]
19. Schwarz EM, Benz EB, Lu AP, et al. Quantitative small-animal surrogate to evaluate drug efficacy in preventing wear debris-induced osteolysis. J Orthop Res. 2000; 18:849–855. [PubMed: 11192243]
20. Tsutsumi R, Hock C, Bechtold CD, et al. Differential effects of biologic versus bisphosphonate inhibition of wear debris-induced osteolysis assessed by longitudinal micro-CT. J Orthop Res. 2008; 26:1340–1346. [PubMed: 18404739]
21. Tsutsumi R, Xie C, Wei X, et al. PGE2 signaling through the EP4 receptor on fibroblasts upregulates RANKL and stimulates osteolysis. J Bone Miner Res. 2009; 24:1753–1762. [PubMed: 19419302]
22. Childs LM, Paschalis EP, Xing L, et al. In vivo RANK signaling blockade using the receptor activator of NF-kappaB:Fc effectively prevents and ameliorates wear debris-induced osteolysis via osteoclast depletion without inhibiting osteogenesis. J Bone Miner Res. 2002; 17:192–199. [PubMed: 11811549]
23. Ito H, Koefoed M, Tiyapatanaputi P, et al. Remodeling of cortical bone allografts mediated by adherent rAAV-RANKL and VEGF gene therapy. Nat Med. 2005; 11:291–297. [PubMed: 15711561]
24. D'Antonio JA, Capello WN, Ramakrishnan R. Second-generation annealed highly cross-linked polyethylene exhibits low wear. Clin Orthop Relat Res. 2012; 470:1696–1704. [PubMed: 22161120]
25. Amstutz HC, Takamura KM, Ebramzadeh E, et al. Highly cross-linked polyethylene in hip resurfacing arthroplasty: long-term follow-up. Hip Int. 2015; 25:39–43. [PubMed: 25362872]
26. Martell JM, Berdia S. Determination of polyethylene wear in total hip replacements with use of digital radiographs. J Bone Joint Surg Am. 1997; 79:1635–1641. [PubMed: 9384422]
27. Looney RJ, Boyd A, Totterman S, et al. Volumetric computerized tomography as a measurement of periprosthetic acetabular osteolysis and its correlation with wear. Arthritis Res. 2002; 4:59–63. [PubMed: 11879538]
28. Howie DW, Neale SD, Stamenkov R, et al. Progression of acetabular periprosthetic osteolytic lesions measured with computed tomography. J Bone Joint Surg Am. 2007; 89:1818–1825. [PubMed: 17671023]
29. Schwarz EM, Campbell D, Totterman S, et al. Use of volumetric computerized tomography as a primary outcome measure to evaluate drug efficacy in the prevention of peri-prosthetic osteolysis: a 1-year clinical pilot of etanercept vs. placebo. J Orthop Res. 2003; 21:1049–1055. [PubMed: 14554218]

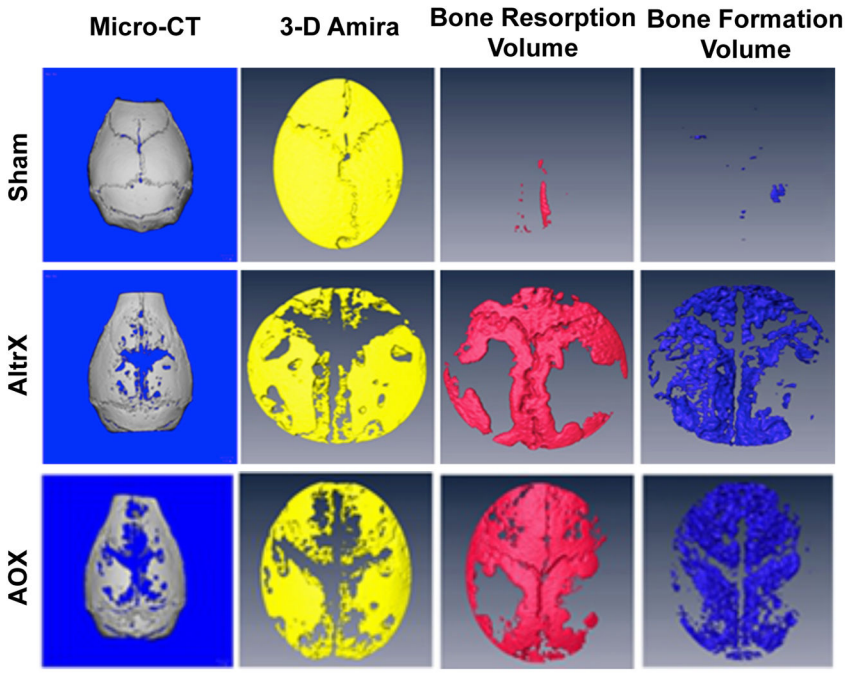

Figure 1. Volumetric micro-CT and Amira analyses of UHMWPE particle induced bone resorption and bone formation

3D renderings of representative calvaria from the Sham, AltrX and AOX treatment groups are show to illustrate volumetric assessment of bone resorption and bone formation in this study. The primary reconstructed Micro-CT scans of Day 10 calvaria reveal the persistent mature highly mineralized bone that was present prior to surgery, and the bone voids represent regions that have undergone particle-induced bone remodeling. Co-registration of the high and low mineralized calvaria tissue from the Day 0 and Day 10 micro-CT scans in Amira allows for visualization of osteolysis from baseline (void region in the yellow image). Subtraction of the Day 10 from the Day 0 high mineralized bone volume reveals the Bone Resorption Volume (red), and the low density mineralized tissue in Day 10 calvaria reveals the Bone Formation Volume (blue). Note the very limited bone remodeling in Sham, and that most of the Bone Resorption Volume in both particle groups has been filled with new bone.

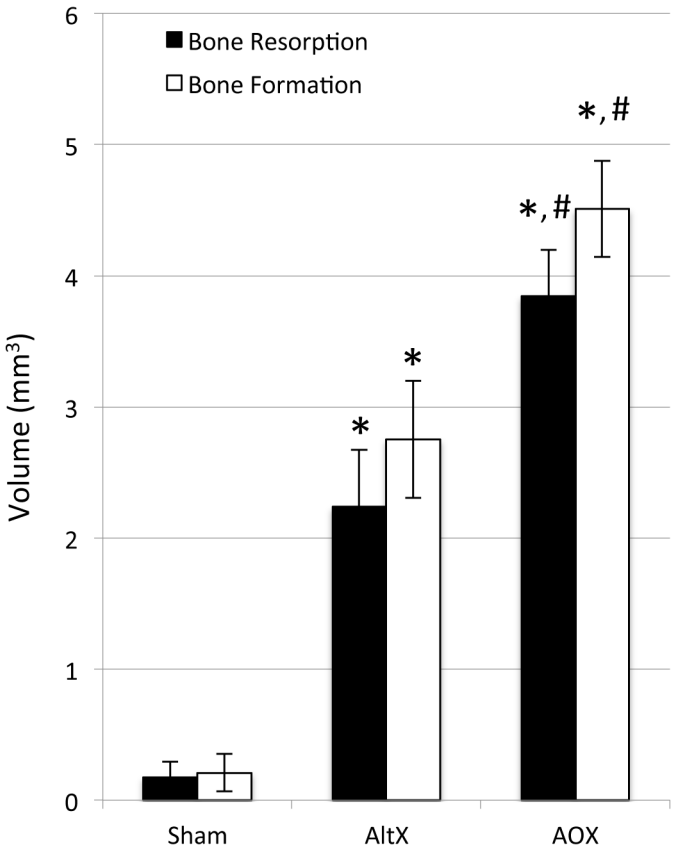

Figure 2. Antioxidant increases UHMWPE particle induced bone resorption and bone formation

The Bone Resorption Volume and Bone Formation Volume in the calvaria of Sham, AltrX and AOX treated mice (n=10) were quantified as described in Figure 1, and the data are presented as the mean +/− SD (*p<0.001 vs. Sham; #p<0.001 vs. AltrX).

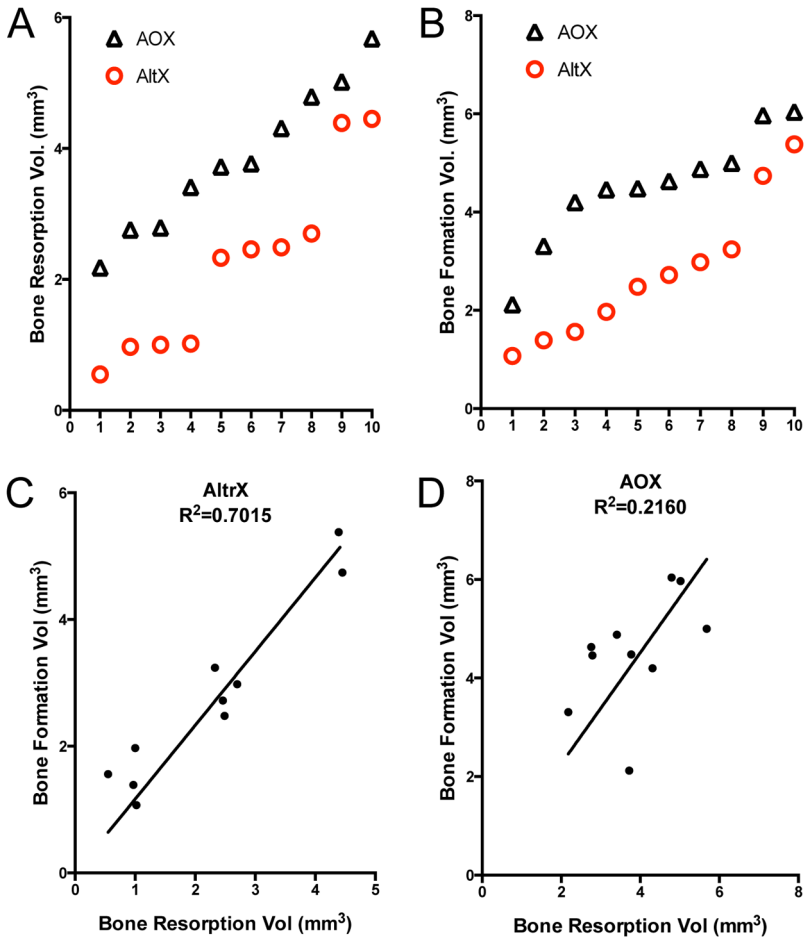

Figure 3. Antioxidant improves the osteolytic:osteogenic potential of UHMWPE particles

The data in Figure 2 were further analyzed to assess the differences between AltrX and AOX via rank order (A, B), and to define the relative bone osteolytic:osteogenic potential of both particles via linear regression (C,D). The results confirm that AOX particles stimulate more bone resorption and new bone formation versus AltrX ($p<0.002$ via Wilcoxon signed rank test). The results also demonstrate that osteoclast-osteoblast coupling is virtually perfect in AltrX treated calvaria (Slope=0.97, $R^2=0.7015$, $p<0.0001$). While this response was more variable in AOX treated mice, the results demonstrate that these particles stimulate more bone formation than bone resorption as indicated by the positive slope (Slope=1.13, $R^2=0.2160$, $p<0.001$).

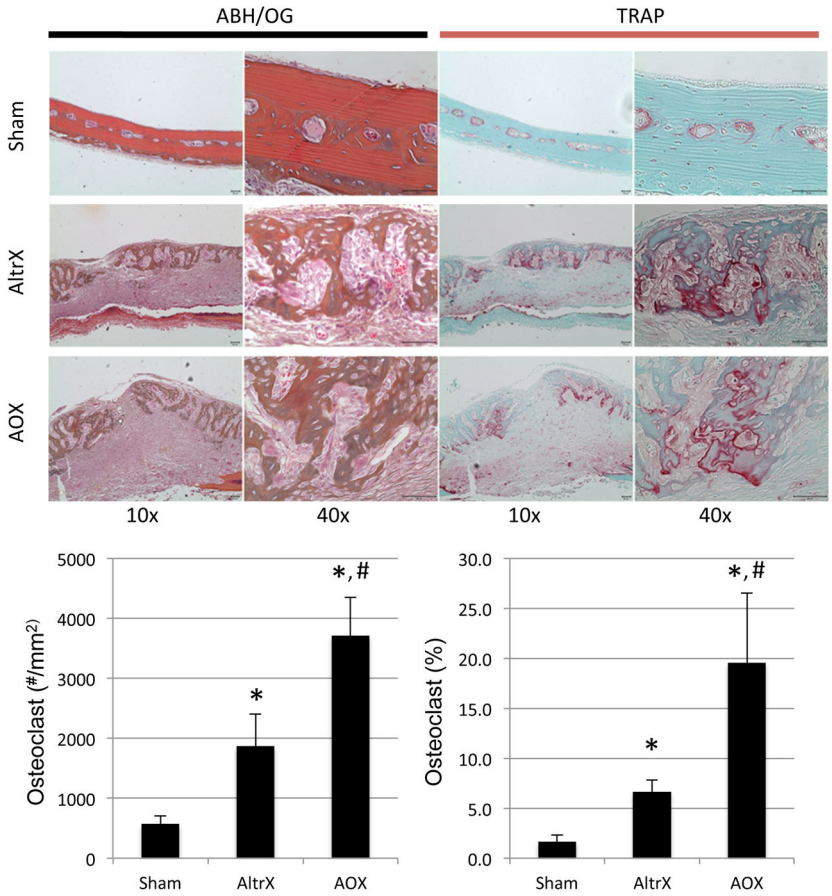

Figure 4. Antioxidant increases UHMWPE particle-induced osteoclast numbers

Alcian blue hematoxylin/orange G (ABH/OG) and tartrate resistant acid phosphatase (TRAP) stained demineralized histology of the calvaria described in Figure 1 are presented at 10x and 40x magnification to illustrate the absence of remodeling in Sham, and the extensive remodeling in both AltrX and AOX treated calvaria. Histomorphometry was performed to quantify osteoclast numbers and the percent of TRAP+ bone surface in the calvaria (n=5), and the data are presented as the mean +/− SD (*p<0.001 vs. Sham; #p<0.001 vs. AltrX).

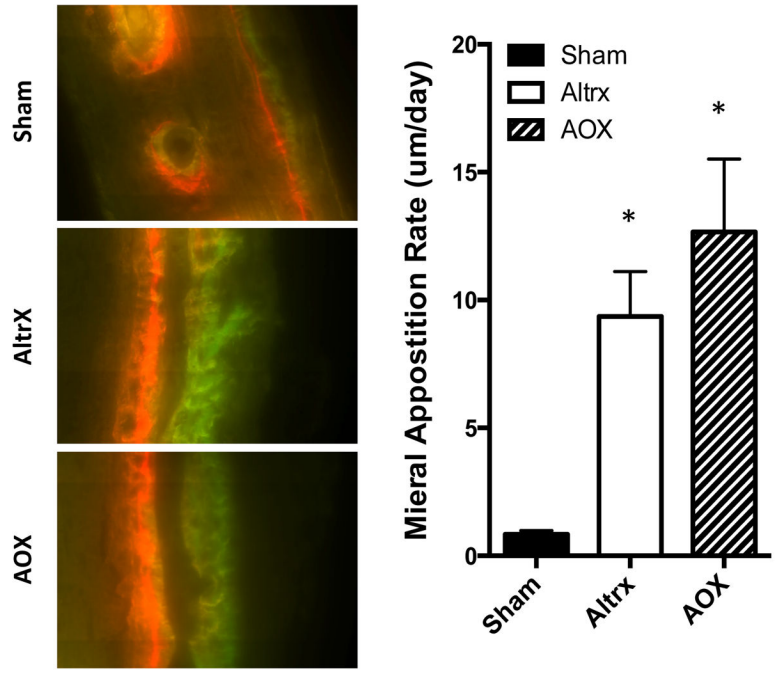

Figure 5. UHMWPE particle-induced mineral apposition rates

Half of tissue of the calvaria described in Figure 4 were processed for undemineralized histology, and representative fluorescent images obtained at 100 X magnification are shown to illustrated the alizarin red and calcein green double labels measured to quantify the mineral apposition rates MAR. Note the significantly greater MAR in the particle treated calvaria (*p<0.001 vs. sham; p=0.2444, AOX vs. Altrx).

Table 1

The characteristics of GUR 1020 (AltrX) and AOX 115 kGy particles

Material	GUR 1020, 75 kGy, Remelted	AOX 115 kGy
Median Particle Size	0.9 um (range 0.47–38.32 um)	0.9 um (range 0.55–30.85 um)
Mean Particle Size	2.1 um (range 0.47–38.32 um)	2.1 um (range 0.55–30.85 um)
Average Aspect Ratio	1.94 (range 1.04–7.74)	1.76 (range 1.03–6.86)
Average Roundness	0.57 (range 0.13–0.96)	0.62 (range 0.15–0.97)
Average Form Factor	0.67 (range 0.07–1.11)	0.69 (range 0.09–1.01)
Average Perimeter	9.1 um (range 1.58–326.50 um)	9.1 um (range 1.84–186.05 um)